

Diastereoselective Formation of Chiral Tris-Cyclometalated Iridium (III) Complexes: Characterization and Photophysical Properties

Christine Schaffner-Hamann,[†] Alexander von Zelewsky*^{†,‡} Andrea Barbieri,[‡] Francesco Barigelletti,[‡] Gilles Muller,[§] James P. Riehl,[§] and Antonia Neels^{||}

Contribution from the Department of Chemistry, University of Fribourg, Pérolles, CH-1700 Fribourg, Switzerland, Istituto ISOF-CNR, Via P. Gobetti 101, 40129 Bologna, Italy, Department of Chemistry, University of Minnesota, Duluth, Minnesota 55812-3020, and Institute of Chemistry, University of Neuchâtel, Av. Bellevaux 51, CH-2000 Neuchâtel, Switzerland

Received March 9, 2004; E-mail: Alexander.vonzewelsky@unifr.ch

Abstract: Chiral, facial tris-cyclometalated Ir(III) complexes, *fac*- Δ -Ir(pppy)₃, *fac*- Λ -Ir(pppy)₃, *fac*- Λ -IrL (where pppy is (8*R*,10*R*)-2-(2'-phenyl)-4,5-pinenopyridine and L is a tripodal ligand comprising three pppy moieties connected through a mesityl spacer) have been synthesized and characterized. In IrL, NMR and CD studies indicate that only one diastereomer is formed, with the Λ configuration at the metal center, whereas enantiopure pppy yields the *fac*- Λ - and the *fac*- Δ -stereoisomer in a ratio 2:3. *fac*- Λ -IrL was structurally characterized using X-ray crystallography. The luminescence properties including CPL, of the three complexes and their sensitivity to dioxygen were examined.

Introduction

The optical properties of transition metal complexes, especially the d⁶ Ru(II), Os(II), Rh(III), and Ir(III) species, have been studied by a wide variety of spectroscopic approaches.^{1,2} In particular, the luminescent and photophysical properties of related tris-chelate Ir(III) complexes have been the object of detailed studies.^{1,3,4} Ir(III) complexes can be prepared with either diimine ligands or cyclometalated ligands, such as 2-phenylpyridine (ppy)^{3–5} and the tris-chelate complexes with this formally monoanionic ligand are isoelectronic with the cationic tris-diimine complexes of Ru(II) and Os(II). Compared to Ru(II) and Os(II) complexes, the diimine d⁶ Ir(III) complexes exhibit

longer excited-state lifetimes (τ on microsecond time scale) and higher luminescence efficiencies ($\Phi \approx 10^{-1}$ – 10^{-2}) in fluid solutions, at room temperature.^{1–6} The luminescence yields are found to be even higher for Ir(pppy)₃ and related complexes, in some cases with $\Phi > 0.5$.^{5–7} Also for this reason, Ir(III) cyclometalated complexes are receiving a great deal of attention as efficient phosphor dopant in polymer matrix for applications in the area of organic light emitting diode devices (OLEDs).⁷ Recently,⁸ we described the synthesis of a chiral tripodal ligand based on bipyridine units and the study of its coordination with ruthenium (II) and iron (II). It was demonstrated that this ligand enables the formation of octahedral complexes with predetermined configuration at the metal center with complete stereoselectivity. Bis-cyclometalated complexes of rhodium (III) were also described using chiral ligands,⁹ but less attention has been devoted till now to iridium (III) tris-cyclometalated complexes in diastereoselective synthesis. Here, we describe the formation,

[†] University of Fribourg.

[‡] Istituto ISOF-CNR.

[§] University of Minnesota Duluth.

^{||} University of Neuchâtel.

- (1) (a) Balzani, V.; Juris, A.; Venturi, M.; Campagna, S.; Serroni, S. *Chem. Rev.* **1996**, *96*, 759–833. (b) Maestri, M.; Balzani, V.; Deuschel-Cornioley, C.; von Zelewsky, A. *Adv. Photochem.* **1992**, *17*, 1–68. (c) Dixon, I. M.; Collin, J.-P.; Sauvage, J.-P.; Flamigni, L.; Encinas, S.; Barigelletti, F. *Chem. Soc. Rev.* **2000**, *29*(6), 385–391.
- (2) (a) Vlcek, A., Jr. *Coord. Chem. Rev.* **1998**, *177*, 219–256. (b) Demadis, K. D.; Hartshorn, C. M.; Meyer, T. J. *Chem. Rev.* **2001**, *101*, 2655–2685. (c) Demas, J. N.; DeGraff, B. A. *Coord. Chem. Rev.* **2001**, *211*, 317–351.
- (3) (a) Shaw, J. R.; Sadler, G. S.; Wacholtz, W. F.; Ryu, C. K.; Schmehl, R. H. *New J. Chem.* **1996**, *20*, 749–758. (b) Sprouse, S.; King, K. A.; Spellane, P. J.; Watts, R. J. *J. Am. Chem. Soc.* **1984**, *106*, 6647–6653. (c) King, K. A.; Spellane, P. J.; Watts, R. J. *J. Am. Chem. Soc.* **1985**, *107*, 1431–1432. (d) Ohsawa, Y.; Sprouse, S.; King, K. A.; DeArmond, M. K.; Hanck, K. W.; Watts, R. J. *J. Phys. Chem.* **1987**, *91*, 1047–1054. (e) Ichimura, K.; Kobayashi, T.; King, K. A.; Watts, R. J. *J. Phys. Chem.* **1987**, *91*, 6104–6106.
- (4) (a) Garces, F. O.; King, K. A.; Watts, R. J. *Inorg. Chem.* **1988**, *27*, 3464–3471. (b) Garces, F. O.; Watts, R. J. *Inorg. Chem.* **1990**, *29*, 582–584. (c) Wilde, A. P.; King, K. A.; Watts, R. J. *J. Phys. Chem.* **1991**, *95*, 629–634. (d) Tamayo, A. B.; Alleyne, B. D.; Djurovich, P. I.; Lamansky, S.; Tsyba, I.; Ho, N. N.; Bau, R.; Thompson, M. E. *J. Am. Chem. Soc.* **2003**, *125*, 7377–7387. (e) Colombo, M. G.; Hauser, A.; Guedel, H. U. *Inorg. Chem.* **1993**, *32*, 3088–3092. (f) Colombo, M. G.; Brunold, T. C.; Riedener, T.; Guedel, H. U.; Fortsch, M.; Buergi, H.-B. *Inorg. Chem.* **1994**, *33*, 545–550.

- (5) (a) Dedeian, K.; Djurovich, P. I.; Garces, F. O.; Carlson, G.; Watts, R. J. *Inorg. Chem.* **1991**, *30*, 1685–1687. (b) Nazeeruddin, M. K.; Humphry-Baker, R.; Berner, D.; Rivier, S.; Zuppiroli, L.; Graetzel, M. *J. Am. Chem. Soc.* **2003**, *125*, 8790–8797. (c) Tsuboyama, A.; Iwakaki, H.; Furugori, M.; Mukaide, T.; Kamatani, J.; Igawa, S.; Moriyama, T.; Miura, S.; Takiguchi, T.; Okada, S.; Hoshino, M.; Ueno, K. *J. Am. Chem. Soc.* **2003**, *125*, 12 971–12 979.
- (6) (a) Schmid, B.; Garces, F. O.; Watts, R. J. *Inorg. Chem.* **1994**, *33*, 9–14. (b) Neve, F.; Crispini, A.; Campagna, S.; Serroni, S. *Inorg. Chem.* **1999**, *38*, 2250–2258. (c) Lamansky, S.; Djurovich, P.; Murphy, D.; Abdel-Razzaq, F.; Kwong, R.; Tsyba, I.; Bortz, M.; Mui, B.; Bau, R.; Thompson, M. E. *Inorg. Chem.* **2001**, *40*, 1704–1711.
- (7) (a) Baldo, M. A.; O'Brien, D. F.; You, Y.; Shoustikov, A.; Sibley, S.; Thompson, M. E.; Forrest, S. R. *Nature* **1998**, *395*, 151–154. (b) Baldo, M. A.; Lamansky, S.; Burrows, P. E.; Thompson, M. E.; Forrest, S. R. *Appl. Phys. Lett.* **1999**, *75*, 4–6. (c) Adachi, C.; Baldo, M. A.; Forrest, S. R.; Thompson, M. E. *Appl. Phys. Lett.* **2000**, *77*, 904–906. (d) Sudhakar, M.; Djurovich, P. I.; Hogen-Esch, T. E.; Thompson, M. E. *J. Am. Chem. Soc.* **2003**, *125*, 7796–7797. (e) Grushin, V. V.; Herron, N.; LeCloux, D. D.; Marshall, W. J.; Petrov, V. A.; Wang, Y. *Chem. Commun.* **2001**, 1494–1495.
- (8) Hamann, C.; von Zelewsky, A.; Neels, A.; Stoeckli-Evans, H. *Dalton* **2004**, 402–406.

characterization, absorption, and luminescence properties (including circularly polarized luminescence, CPL) of facial mononuclear Ir(III) complexes comprising three chiral cyclo-metalating didentate ligands, which are derivatives of phenylpyridine. Two diastereoisomers of the tris-didentate complex with (8*R*,10*R*)-2-(2'-phenyl)-4,5-pinenopyridine (pppy), as well as a single stereoisomer of a related tripodal ligand (**L**) are investigated.

Experimental Section

General. NMR spectra were recorded on a Varian Gemini-300 (for 300 MHz NMR) or on a Bruker Advance DRX400 (for 400 MHz NMR) spectrometers. Chemical shifts are given in ppm using the solvent as internal standard. Mass spectral data (ESI and HRMS) were acquired on a Bruker FTMS 4.7 T BioApex II. Circular dichroism (CD) spectra were recorded on a Jasco J-715 spectropolarimeter. Electrochemical measurements were carried out at room temperature using a PAR 273A electrochemical analysis system with 270 research electrochemistry software. Cyclic voltammograms were obtained in butyronitrile, using a microcell equipped with a stationary platinum disk electrode with tetra-*n*-butylammonium hexafluorophosphate (0.1 M) as base electrolyte. Ru(bpy)₃²⁺ was used as the standard, taking the oxidation potential as +1.26 V, vs SCE.¹⁰ Half-wave potentials were calculated as an average of the cathodic and anodic peak. UV/Visible spectra for acetonitrile or CH₂Cl₂ solutions were measured on a Perkin-Elmer Lambda 40 spectrometer. The steady-state luminescence spectra for air-equilibrated and freeze-pump-thaw degassed dilute (ca. 2 × 10⁻⁵ M) acetonitrile solutions of the investigated complexes were measured using a Perkin-Elmer LS 50B spectrometer or a Spex Fluorolog spectrometer, equipped with a Hamamatsu R928 tube; an excitation wavelength of 350 nm was used. Luminescence quantum yields at room temperature (Φ) were evaluated by comparing wavelength-integrated intensities (*I*) with reference to [Ru(bpy)₃]Cl₂ (Φ_r = 0.028 in air-equilibrated water¹¹), and quinine sulfate (Φ_r = 0.546 in 1 N H₂SO₄¹²) as standards and by using the following equation¹³

$$\Phi = \Phi_r \frac{A_r n^2 I}{A n_r^2 I_r}$$

where *A* and *n* are absorbance values (ca. 0.1) at the employed excitation wavelength and refractive index of the solvent, respectively. Measurements at 77 K were conducted by employing capillary tubes immersed in liquid nitrogen and hosted within homemade quartz dewars. Band maxima and relative luminescence intensities were obtained with uncertainty of 2 nm and 20%, respectively. The luminescence lifetimes were obtained with an IBH 5000F single-photon equipment by using a 375 nm nanoled excitation source. Analysis of the luminescence

decay profiles against time was accomplished by using software provided by the manufacturer. The lifetime values are obtained with an estimated uncertainty of 10%. The circularly polarized luminescence and total luminescence spectra were recorded on an instrument described previously, operating in a differential photon-counting mode.¹⁴ The excitation source was a 450-watt xenon continuous wave arc lamp of a SPEX Fluorolog 2 spectrofluorimeter. The dispersion of the excitation and emission monochromators (SPEX 1681B) was 4 nm/mm. The measurements were performed in dry acetonitrile solutions at concentrations of 1 × 10⁻⁴ M at 295 K.

Materials. Oxygen- or water-sensitive reactions were conducted under a positive pressure of argon in oven-dried glassware, using Schlenk techniques. Unless otherwise stated, commercial grade reagents (spectroscopic grade when needed) were used without further purification. 1,3,5-tris-bromomethylbenzene,¹⁵ (8*R*,10*R*)-2-(2'-phenyl)-4,5-pinenopyridine (pppy),^{9c} 2-(2'-hydroxy)ethyl-2-tetrahydro-2H-pyran ether¹⁶ were prepared according or analogous to the literature methods. Ir(acac)₃ was purchased from Strem Chemicals.

X-ray Crystallography. Suitable orange single crystals of fac-Λ-Ir**L** were obtained by slow diffusion of acetone solution of the complex in water at room temperature. Data were measured at -120 °C using Mo-Kα radiation (λ = 0.710 73 Å) with a Stoe Mark II-Imaging Plate Diffractometer System (Stoe & Cie, 2002)¹⁷ equipped with a graphite-monochromator. The structure was solved by direct methods using the program SHELXS-97.¹⁸ The refinement and all further calculations were carried out using SHELXL-97.¹⁹ One O-C-C-O fragment is disordered over 2 positions and both parts (half occupied) are refined with constrained bond distances to their theoretical values (C-O = 1.41; C-C = 1.52). Two acetone molecules, one occupies a special position, were found per asymmetric unit. Both of them are half occupied and refined isotropically. The hydrogen atoms were included in calculated positions and treated as riding atoms using SHELXL-97 default parameters. The non-H atoms were refined anisotropically, using weighted full-matrix least-squares on F². An absorption correction was applied using DIFABS (*T*_{min} = 0.313, *T*_{max} = 0.748).

Precursor 1. In a 150 mL flask fitted with condenser, dropping funnel and argon inlet was flushed with argon and then charged with 2-(2'-hydroxy)ethyl-2-tetrahydro-2H-pyran ether (1.9 g, 0.01 mol), ground sodium hydroxide (0.4 g, 0.01 mol), tetrabutylammonium hydrogensulfate (0.13 g, 0.4 mmol) and dry THF (70 mL). The mixture was then stirred at room temperature during 1 h. 1,3,5-tris-bromomethylbenzene (0.9 g, 0.0025 mol) in THF (20 mL) was added slowly and the mixture heated to reflux for 3 h. A white precipitate appeared. The solution was then cooled, filtered and the solvent was removed to leave a yellow oil. This oil was dissolved in CH₂Cl₂, and the organic layer was washed with water. The organic phase was dried over MgSO₄, filtered and evaporated to dryness. The

(9) (a) Ghizdavu, L.; Kolp, B.; Von Zelewsky, A.; Stoeckli-Evans, H. *Eur. J. Inorg. Chem.* **1999**, 1271–1279. (b) Ghizdavu, L.; Von Zelewsky, A.; Stoeckli-Evans, H. *Eur. J. Inorg. Chem.* **2001**, 993–1003. (c) Ghizdavu, L.; Lentzen, O.; Schumm, S.; Brodtkorb, A.; Moucheron, C.; Kirsch-De Mesmaeker, A. *Inorg. Chem.* **2003**, 42, 1935–1944.
(10) (a) Lin, C. T.; Boettcher, W.; Chou, M.; Creutz, C.; Sutin, N. *J. Am. Chem. Soc.* **1976**, 98, 6536–6544. (b) Juris, A.; Balzani, V.; Belser, P.; Von Zelewsky, A. *Helv. Chim. Acta* **1981**, 64, 2175–2182. (c) Sutin, N.; Creutz, C. *Adv. Chem. Ser.* **1978**, 168, 1–27.
(11) Nakamaru, K. *Bull. Chem. Soc. Jpn.* **1982**, 55, 2697–2705.
(12) Meech, S. R.; Phillips, D. *J. Photochem.* **1983**, 23, 193–217.
(13) Crosby, G. A.; Demas, J. N. *J. Phys. Chem.* **1971**, 75, 991–1024.

(14) Riehl, J. P.; Muller, G. In *Handbook on the Physics and Chemistry of Rare Earths*; Gschneidner, K. A., Buznli, J.-C. G., Pecharsky, V. K., Eds.; North-Holland Publishing Company: Amsterdam, 2004, Vol. 34, in press.
(15) Newkome, G. R.; Yao, Z.; Baker, G. R.; Gupta, V. K.; Russo, P. S.; Saunders, M. J. *J. Am. Chem. Soc.* **1986**, 108, 849–850.
(16) Kyba, E. P.; Helgeson, R. C.; Madan, K.; Gokel, G. W.; Tarnowski, T. L.; Moore, S. S.; Cram, D. J. *J. Am. Chem. Soc.* **1977**, 99, 2564–2571.
(17) Stoe & Cie 2002. *X-Area V1.17 & X-RED32 V1.04 Software*. Stoe & Cie GmbH, Darmstadt, Germany.
(18) G. M. Sheldrick, 1990, **A46**, 467.
(19) G. M. Sheldrick, *Universität Göttingen, Germany*, **1999**.

residue was purified by column chromatography (SiO₂, eluent: hexane/EtOAc 1:1 to EtOAc) to give **1** as a colorless oil (1.05 g, 60%). ¹H NMR (300 MHz, CDCl₃): δ 7.21 (s, 3H, H_α); 4.61 (m, 3H, H_{a'}); 4.53 (s, 6H, H_e); 3.83 (m, 6H, H_{c'}); 3.70–3.40 (m, 24H, H_{a,b,c,d}); 1.90–1.42 (m, 18H, H_{b',c',d'}). ¹³C NMR (100 MHz, CDCl₃): δ 139.1; 126.6; 99.3; 73.5; 71.1; 70.0; 67.1; 62.6; 60.8; 31.0; 25.8; 19.9. ESI-MS calcd. for C₃₆H₆₀NaO₁₂ [M+Na⁺] 707.40, found 707.41.

Precursor 2. To a solution of **1** (1.05 g, 1.53 mmol) dissolved in 50 mL of a mixture CH₂Cl₂/MeOH (1:1) were added 2 drops of HCl 37%. The solution was stirred at room-temperature overnight. NaHCO₃ was then added and the solvents were removed. The crude product was taken up into EtOAc, filtered and evaporated to dryness to leave an oil whose purity was good enough (>95% by NMR) to be used without purification. ¹H NMR (300 MHz, CDCl₃): δ 7.22 (s, 3H, H_α); 4.55 (s, 6H, H_e); 3.71–3.57 (m, 24H, H_{a,b,c,d}). ¹³C NMR (100 MHz, CDCl₃): δ 139.0; 126.7; 73.4; 73.0; 70.9; 70.0; 62.2. ESI-MS calcd. for C₂₁H₃₆NaO₉ [M+Na⁺] 451.23, found 451.26.

Precursor 3. A solution of the triol **2** (0.615 g, 1.42 mmol) in 50 mL of anhydrous CH₂Cl₂, in the presence of freshly distilled triethylamine (5 mL) was cooled to –5 °C under argon. A solution of mesyl chloride (0.8 mL, 10 mmol) in 10 mL of anhydrous CH₂Cl₂ was added dropwise to the previous solution. The temperature was maintained below 0 °C as the reaction is very exothermic. After 3 h stirring at –5 °C, the mixture was brought to room temperature. The reaction mixture was washed with H₂O and dried over MgSO₄. Due to the instability of the compound on column, it was used without purifications in the next step. ¹H NMR (300 MHz, CDCl₃): δ 7.23 (s, 3H, H_α); 4.51 (s, 6H, H_e); 4.36 (m, 6H, H_a); 3.75 (m, 6H, H_b); 3.63 (m, 12H, H_{c,d}).

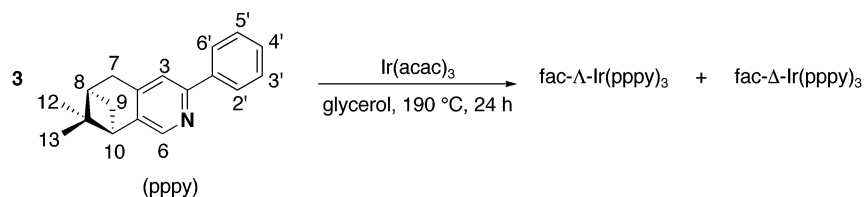
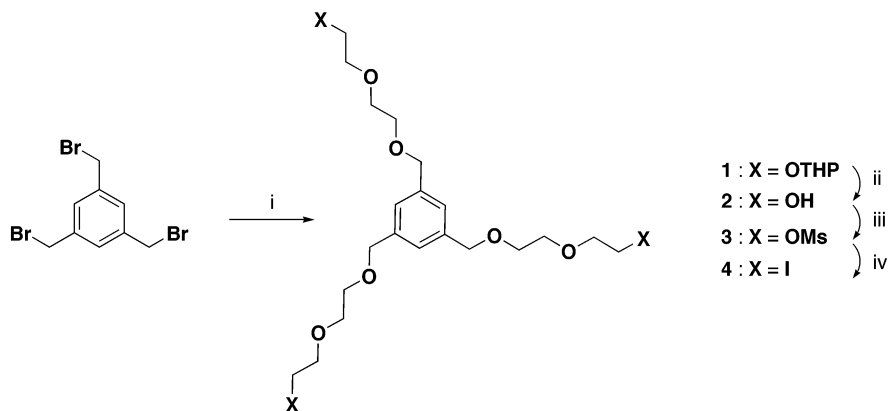
Precursor 4. Crude **3** was dissolved in acetonitrile (80 mL) and NaI (9 g, 60 mmol) was added. The yellow mixture was then heated at 80 °C for 8 h. After the solvent was removed, the residue was taken up into H₂O/CH₂Cl₂. Extraction with CH₂Cl₂ and drying over MgSO₄ left, after evaporation of the solvent, a brown oil which was filtered on alumina (eluent hexane/EtOAc 1:1) to give the product as a colorless oil (0.463 g, 43% from the triol). ¹H NMR (300 MHz, CDCl₃): δ 7.23 (s, 3H, H_α); 4.56 (s, 6H, H_e); 3.77–3.63 (m, 18H, H_{b,c,d}); 3.27 (t, 6H, H_a). ¹³C NMR (100 MHz, CDCl₃): δ 139.0; 126.7; 73.6; 72.4; 70.7; 70.0; 3.3. ESI-MS calcd. for C₂₁H₃₃I₃NaO₆ [M+Na⁺] 784.93, found 784.96.

Ligand (–)-(7S,10R)-L. To a freshly prepared solution of LDA (7 mmol in THF) cooled to –20 °C, was added a degassed solution of (8R,10R)-2-(2'-phenyl)-4,5-pinenopyridine (1.2 g, 4.8 mmol in anhydrous THF) over 40 min. The reaction medium was then warmed to 0 °C for 3 h. The solution turned progressively dark red; then **4** (0.41 g, 0.53 mmol) dissolved in dry THF (10 mL) was added. The mixture was stirred overnight, and the reaction was quenched with water (2 mL). After evaporation of the THF in a vacuum, the residue was taken up in a CH₂Cl₂/H₂O mixture and the organic layer was dried over MgSO₄ and filtered. Following removal of the solvent, the residue was purified by column chromatography (SiO₂, hexane/EtOAc 5:1 to 1:1) and then by silica preparative plate (hexane/EtOAc 3:1). **5** was obtained as a white powder in 56% yield (0.336 g). ¹H NMR (400 MHz, CDCl₃): δ 8.23 (s, 3H, H₃), 7.97 (d, 6H, H_{2',6'}), 7.65 (s, 3H, H₆), 7.47 (dd, 6H, H_{3',5'}), 7.39

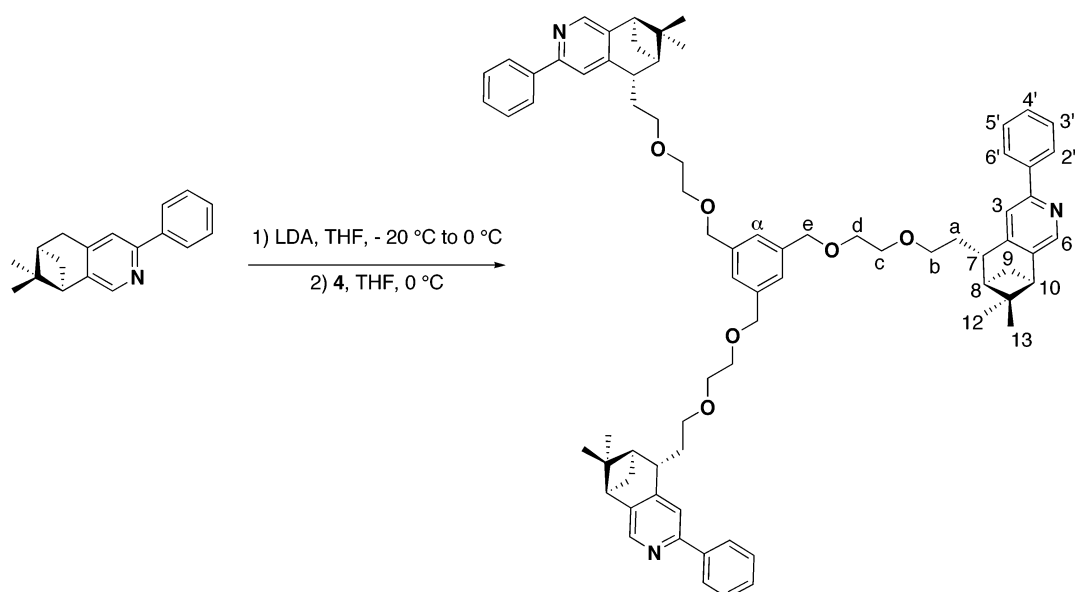
(dd, 3H, H_{4'}), 7.27 (s, 3H, H_α), 4.57 (s, 6H, H_e), 3.66–3.22 (m, 18H, H_{b,c,d}), 3.17 (ddd, 6H, H₇), 2.86 (m, 3H, H₁₀), 2.58 (ddd, 3H, H_{9,exo}), 2.30–2.25 (m, 3H, H_{8,aendo}), 1.85 (m, 3H, H_{a,exo}) 1.44 (s, 9H, H₁₃), 1.28 (d, 3H, H_{9,endo}), 0.65 (s, 9H, H₁₂). ¹³C NMR (100 MHz, CDCl₃): δ 156.3; 149.6; 146.2; 141.3; 140.3; 139.0; 129.0; 128.8; 127.1; 126.7; 119.8; 73.6; 70.8; 70.0; 69.7; 45.3; 44.0; 41.4; 38.3; 34.1; 28.9; 26.7; 21.5. HRMS calcd. for C₇₅H₈₈N₃O₆[M+H]⁺: 1126.66676, found: 1126.66570. UV–vis (λ in nm (ε, M^{–1} cm^{–1}); CH₂Cl₂, 7.6 × 10^{–5} M): 256 (47100); 281 (32900). [α]_D = –130 °, 25 °C, 0.195 g.L^{–1}.

Complexes fac-Δ/Λ-Ir(ppy)₃. Ir(acac)₃ (0.06 g, 0.12 mmol) and (8R,10R)-2-(2'-phenyl)-4,5-pinenopyridine (0.10 g, 0.40 mmol) were dissolved in degassed glycerol (5 mL) and the solution was heated at 190 °C during 24 h. Once the solution is cooled, it was diluted with CH₂Cl₂ and water. The organic layer was washed with water, dried over MgSO₄ and filtered. Following removal of the solvent, the residue was purified by flash chromatography on a silica column using CH₂Cl₂/hexane 1:1 as eluent to yield 39% of a mixture of pure fac-Λ-Ir(ppy)₃ and fac-Δ-Ir(ppy)₃ in the ratio 2:3. The two diastereoisomers were then separated by silica preparative plate (eluent Hexane/EtOAc 5:1) to yield fac-Λ-Ir(ppy)₃ (18 mg) and fac-Δ-Ir(ppy)₃ (25 mg) as bright yellow powders. **fac-Λ-Ir(ppy)₃:** ¹H NMR (400 MHz, acetone d₆): δ 7.86 (s, 3H, H₃); 7.67 (dd, 3H, H₆); 7.19 (s, 3H, H₆); 6.88 (dd, 3H, H_{3'}); 6.78 (ddd, 3H, H_{5'}); 6.72 (ddd, 3H, H_{4'}); 3.15 (m, 6H, H₇); 2.72 (m, 3H, H_{9,exo}); 2.52 (m, 3H, H₁₀); 2.30 (m, 3H, H₈); 1.32 (s, 9H, H₁₃); 1.26 (d, 9H, H_{9,endo}); 0.47 (s, 9H, H₁₂). ¹³C NMR (100 MHz, acetone d₆): δ 165.3; 161.3; 145.2; 145.1; 143.0; 141.4; 137.4; 128.8; 123.6; 119.5; 118.5; 44.8; 40.3; 39.3; 32.8; 32.4; 25.6; 21.1. HRMS calcd. for C₅₄H₅₄Ir N₃ [M]⁺: 937.39414, found: 937.39397. UV–vis (λ in nm (ε, M^{–1} cm^{–1}); CH₂Cl₂, 1.9 × 10^{–5} M): 242 (53 700); 286 (39 200); 342 (12 100); 382 (sh, 9200); 408 (sh, 6800); 452 (sh, 3100); 487 (sh, 1500). Emission (CH₃CN, 2 × 10^{–5} M): excitation 350 nm, emission 505 nm. CD (CH₂Cl₂ λ in nm (Δε) 1.9 × 10^{–5} M): 297 (83); 281 (–20). **fac-Δ-Ir(ppy)₃:** ¹H NMR (400 MHz, acetone d₆): δ 7.86 (s, 3H, H₃); 7.67 (dd, 3H, H₆); 7.16 (dd, 3H, H_{3'}); 6.86–6.77 (m, 9H, H_{4',5',6'}); 3.16 (m, 6H, H₇); 2.61 (m, 3H, H_{9,exo}); 2.33 (m, 6H, H_{8,10}); 1.37 (s, 9H, H₁₃); 1.15 (d, 3H, H_{9,endo}); 0.74 (s, 9H, H₁₂). ¹³C NMR (100 MHz, acetone d₆): δ 165.5; 131.1; 145.7; 145.0; 142.1; 141.3; 137.6; 129.1; 123.8; 119.7; 118.8; 44.9; 40.2; 39.5; 33.0; 31.5; 25.6; 21.6. HRMS calcd. for C₅₄H₅₄Ir N₃ [M]⁺: 937.394 14, found: 937.394 08. UV–vis (λ in nm (ε, M^{–1} cm^{–1}); CH₂Cl₂, 2.3 × 10^{–5} M): 242 (42 400); 285 (31 900); 334 (sh, 9600); 385 (sh, 7400); 409 (sh, 5200); 456 (sh, 1800); 488 (sh, 1000). Emission (CH₃CN, 2 × 10^{–5} M): excitation 350 nm, emission 507 nm. CD (CH₂Cl₂ λ in nm (Δε) 1.3 × 10^{–5} M): 297 (–92); 281 (29).

fac-Δ-IrL. Ir(acac)₃ (13 mg, 0.027 mmol) and (–)-(7S,10R)-L (30 mg, 0.027 mmol) were dissolved in degassed ethyleneglycol (300 mL) heated at 140 °C and the solution was then brought to 175 °C during 24 h and under vigorous stirring. The solvent was then evaporated by trap-to-trap and the residue was purified by silica preparative plate (eluent Hexane/EtOAc 2:1) and then by alumina preparative plate (eluent Hexane/CH₂Cl₂ 1:2) to yield **IrL** as a bright yellow powder (6 mg, 18%) ¹H NMR (400 MHz, acetone d₆): δ 7.94 (s, 3H, H₃), 7.66 (d, 3H, H₆), 7.26 (s, 3H, H₆), 7.05 (dd, 3H, H_{3'}), 6.75 (ddd, 3H, H_{5'}), 6.68 (m, 6H, H_{4',α}), 4.43 (m, 6H, H_e), 3.74–3.53 (m, 18H,

Scheme 1. Syntheses of the Model Complexes *Fac*- Δ -Ir(pppy)₃ and *Fac*- Λ -Ir(pppy)₃**Scheme 2.** Synthesis of the Ligand L

i) HO(CH₂CH₂)O(CH₂CH₂)OTHP, NaOH, THF, 60 °C; ii) HCl, EtOH reflux;
 iii) MsCl, NEt₃, CH₂Cl₂, 0 °C; iv) NaI, CH₃CN reflux



H_{b,c,d}), 3.29 (ddd, 3H, H₇), 2.65 (m, 6H, H_{9_{exo,endo}}), 2.41 (m, 3H, H₁₀), 2.26 (m, 3H, H₈), 2.05 (m, 3H, H_{a_{exo}}), 1.54 (d, 3H, H_{9_{endo}}), 1.39 (s, 9H, H₁₃), 0.43 (s, 9H, H₁₂). HRMS calcd. for C₇₅H₈₄N₃O₆Ir [M]⁺: 1315.598 39, found: 1315.601 35. UV-vis (λ in nm (ϵ , M⁻¹ cm⁻¹); CH₂Cl₂, 4.5 × 10⁻⁶ M): 245 (48 200); 288 (39 700); 348 (9900); 379 (sh, 9300); 408 (sh, 6400); 453 (sh, 2200); 487 (sh, 1100). Emission (CH₃CN, 2 × 10⁻⁵ M): excitation 350 nm, emission 508 nm. CD (CH₂Cl₂ λ in nm ($\Delta\epsilon$) 4.5 × 10⁻⁶ M): 299 (71), 283 (-14).

Results and Discussion

Synthesis. Tris-cyclometalated Ir(III) complexes *fac*- Λ / Δ -Ir(pppy)₃ were prepared in an analogous way to literature

procedure^{5a} using (8*R*,10*R*)-2-(2'-phenyl)-4,5-pinenopyridine (ppy) as the cyclometalating ligand precursor (Scheme 1).

As demonstrated by Thompson,^{4d} the reaction temperature strongly affects the facial/meridional product ratio of the reaction. When temperature is ~190 °C, the facial isomer is the predominant product.

The use of the enantiomerically pure (8*R*,10*R*)-ppy renders the Λ and Δ isomers of the tris-cyclometalated species diastereoisomeric. Separation with ordinary chromatographic methods becomes therefore possible. Preparative thin-layer chromatography gave the *fac*- Λ / Δ isomers in a ratio 2:3. The absolute configuration at the metal center of the major product was

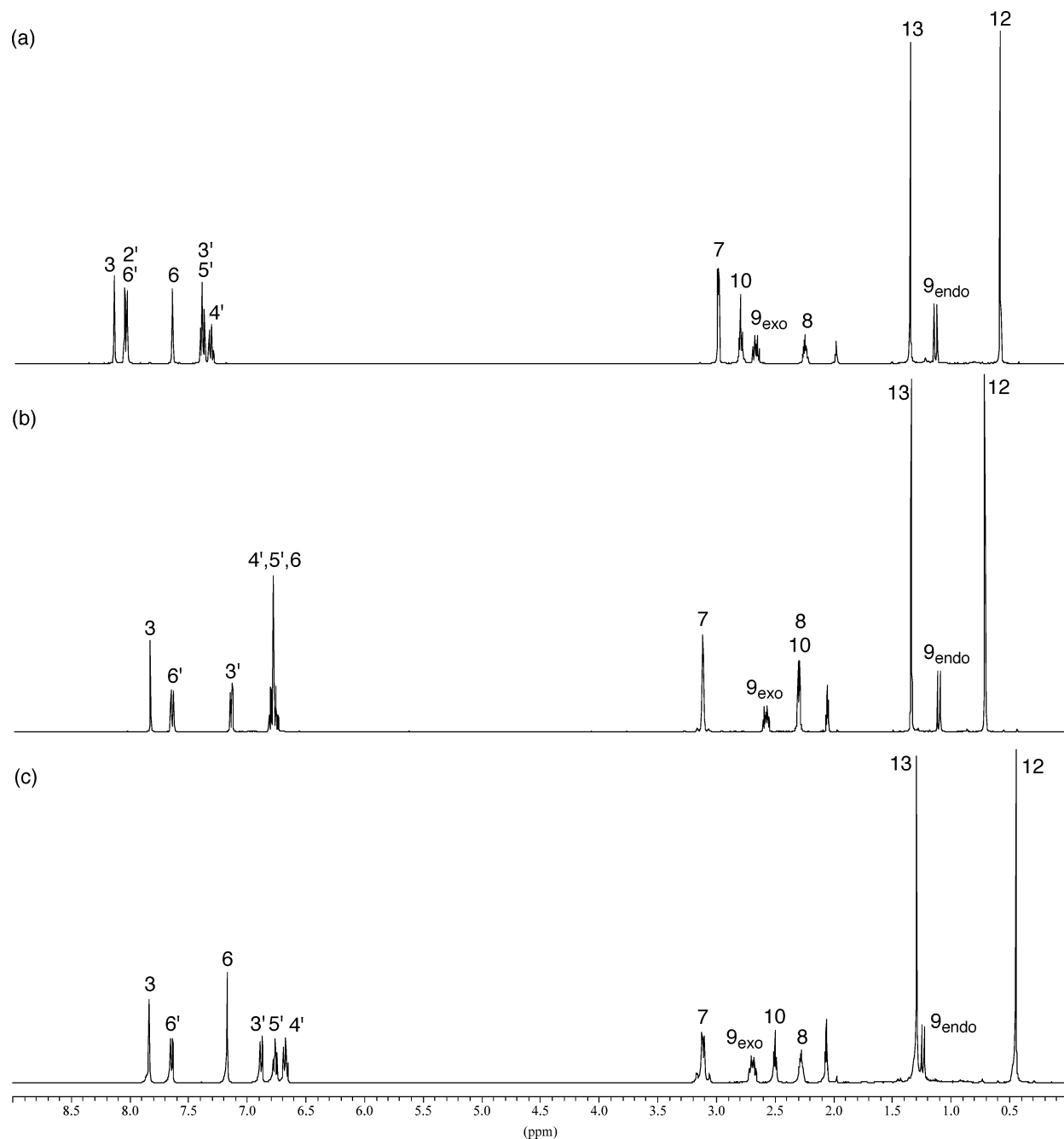


Figure 1. ^1H NMR spectra in acetone d_6 of (a) ligand ppy, (b) complex *fac*- Δ -Ir(ppy) $_3$, and (c) complex *fac*- Λ -Ir(ppy) $_3$ (400 MHz, 298 K).

clearly identified as the Δ isomer: its CD spectrum shows a positive Cotton effect at high energy and a negative one at lower energy which is in full agreement with absolute configuration determined by X-ray crystallography in related complexes with similar ligands.²⁰

The tripodal ligand **L** is obtained in five steps according to a divergent strategy in which the coordinating moieties ppy are connected to the tripod **4** during the last step as shown in Scheme 2.

The tridentate unit **4** is prepared from 1,3,5-tris-bromomethylbenzene in four steps. HO(CH $_2$) $_2$ O(CH $_2$) $_2$ OTHP was reacted with NaOH in the presence of NBu $_4$ HSO $_4$ and to the resulting

alcoholate was then added a solution of 1,3,5-tris-bromomethylbenzene. The tris-THP compound **1** was isolated in 60% yield. The THP protective groups were cleaved by acidic treatment and the resulting triol **2** was converted to the tris-mesylate **3** and subsequently to the tris-iodo compound **4**. **4** was then reacted with 3 equiv. of the anion of ppy (formed by using LDA). The ligand **L** was obtained in 56% yield.

The complex Ir**L** was synthesized from the reaction of Ir(acac) $_3$ with 1 equiv. of **L** in a large volume of ethylenglycol heated at 175 $^\circ\text{C}$. After purification, the complex was obtained in 18% yield.

Polarity. The relative R $_f$ values of the complexes *fac*- Λ -Ir(ppy) $_3$, *fac*- Δ -Ir(ppy) $_3$ and Ir**L** (TLC SiO $_2$, hexane/EtOAc 3:1) are 0.87, 0.80, and 0.17, respectively. Thus, Ir**L** is by far the most polar of the three complexes, whereas *fac*- Δ -Ir(ppy) $_3$,

(20) (a) Hayoz, P.; von Zelewsky, A.; Stoeckli-Evans, H. *J. Am. Chem. Soc.* **1993**, *115*, 5111–5114; Mürner, H. R.; Stoeckli-Evans, H.; von Zelewsky, A. *Inorg. Chem.* **1996**, *35*, 3931–3935.

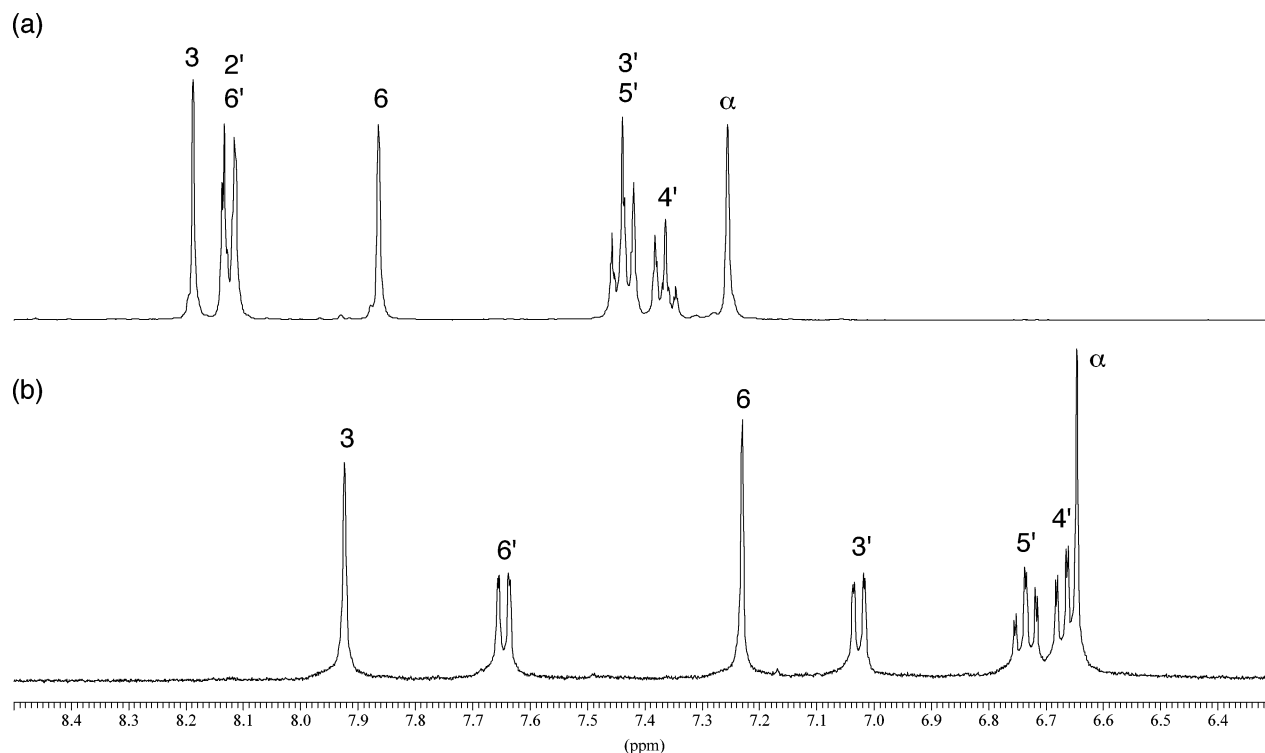


Figure 2. Aromatic region of the ^1H NMR spectra in acetone d_6 of (a) ligand **L** and (b) complex *fac*- Λ -Ir**L** (400 MHz, 298 K).

fac- Λ -Ir(ppy) $_3$, respectively have very similar polarities. Despite this, Ir**L** has the highest solubility in several solvents (hexane, methanol, ether, benzene, etc). This is most probably due to the molecular size. In general, it can be stated, that these coordination compounds behave in many respects as organic molecules of low polarity.

Characterization. NMR. Figure 1 illustrates the ^1H NMR spectra for the free ligand ppy, *fac*- Δ -Ir(ppy) $_3$ and *fac*- Λ -Ir(ppy) $_3$ complexes. These spectra, as well as the ^{13}C NMR spectra, show, in each case, only one set of signals, owing to the high symmetry of these species: therefore the complexes have facial configuration (C_3 symmetry) and the three ligands are thus equivalent. Upon complexation with Ir(III), the signal corresponding to the proton 2' in the free ppy disappears indicating that the cyclometalation occurred.

The ^1H NMR spectrum of the complex Ir**L** is consistent with a facial structure too, but more important, it shows the presence of only one diastereomer. Only one set of signals is observed. A comparison of the aromatic region of the spectra of the free ligand **L** and the Ir**L** is shown in Figure 2.

L shows a set of signals in the aromatic part with chemical shifts ranging from 7.28 to 8.21 ppm. In the complex, these signals lie in the range 6.67–7.94 ppm. A doublet at 7.05 and a triplet at 6.68 ppm are assigned to the protons of the phenyl ring ortho and meta to the metalated carbon atom, respectively 3' and 4'. The protons are high-field shifted compared to **L**: $\Delta\delta = 0.42$ ppm for 3' and $\Delta\delta = 0.71$ ppm for 4'. Upon coordination, the protons 6 are upfield shifted ($\Delta\delta = 0.64$ ppm) because the deshielding effect of the metal center on the proton ortho to the nitrogen atoms is counterbalanced by the shielding effect of the others ppy units. An important point is that the spectrum of Ir**L** is very similar to that of *fac*- Λ -Ir(ppy) $_3$. In fact, it was predicted that the Λ isomer should be formed in the Ir**L** complex, since in our previous work⁸ with analogous

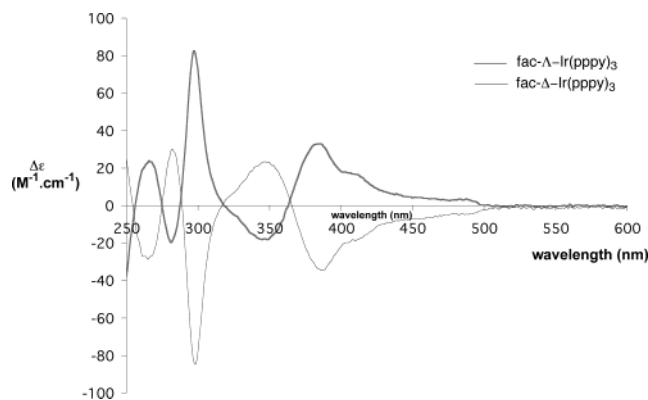


Figure 3. CD spectra of *fac*- Δ -Ir(ppy) $_3$ and *fac*- Λ -Ir(ppy) $_3$ (298 K, in CH_2Cl_2).

tripodal bipyridine ligand (**L'**), only the Λ isomer was obtained in $[\text{RuL}']^{2+}$, as well as in $[\text{FeL}']^{2+}$.

Circular Dichroism, Electrochemistry, and Photophysical Properties. Circular Dichroism. Neither the chiral didentate ligand nor the tripodal ligand show detectable activities in the range 250–600 nm, whereas upon cyclometalation to Ir(III), a strong Cotton effect is observed in all cases. Figure 3 displays the CD spectra of the Λ and Δ diastereoisomers of Ir(ppy) $_3$. The near mirror symmetry of these spectra indicates that the entire CD activity in this spectral range is mainly determined by the chiral configuration at the metal center. The Λ - and Δ -complexes are behaving as pseudo-enantiomers in this respect.

The CD spectrum of Ir**L** (Figure 4) shows clearly that the metal center has a Λ configuration and thus it confirms the analogy between the ^1H NMR spectra of *fac*- Λ -Ir(ppy) $_3$ and *fac*- Λ -Ir**L**.

Electrochemistry. The cyclic voltammograms of the complexes *fac*- Λ -Ir(ppy) $_3$, *fac*- Δ -Ir(ppy) $_3$ and *fac*- Λ -Ir**L** were recorded in butyronitrile. They display reversible couples at

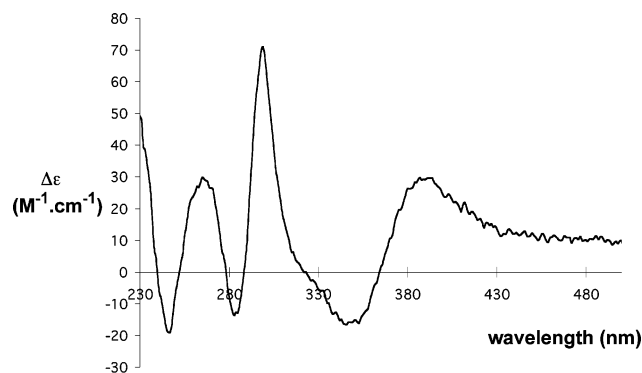


Figure 4. CD spectra of *fac*- Λ -IrL (298 K, in CH_2Cl_2).

Table 1. Absorption and Electrochemical Data of the Studied Complexes

complex	absorption ^a		redox (V/SCE) ^b
	λ (nm)	$\{\epsilon, 10^3 \text{ M}^{-1}\text{cm}^{-1}\}$	$E_{1/2}^{\text{ox}}$
<i>fac</i> - Λ -Ir(pppy) ₃	242 (53.7), 286 (39.2), 342 (12.1), 382 (9.2), 408 (6.8) 452 (3.1), 487 (1.5)		0.52
<i>fac</i> - Δ -Ir(pppy) ₃	242 (42.4), 285 (31.9), 334 (9.6), 385 (7.4), 409 (5.2) 456 (1.8), 488 (1.0)		0.57
<i>fac</i> - Λ -IrL	245 (48.2), 288 (39.7), 348 (9.9), 379 (9.3), 408 (6.4) 453 (2.2), 487 (1.1)		0.49

^a In CH_2Cl_2 or acetonitrile solvents, at 298 K. ^b In butyronitrile, in the conditions used (explored window < -1.80 V), the reduction of the phenylpyridyl-based derivatives is not observed.

+0.52, +0.57, and +0.49 V/SCE, respectively. The data are reported in Table 1. These potentials are assigned to metal-centered Ir^{IV}/Ir^{III} reduction couples. They indicate the relative ease of oxidation in the various species. The pineno-phenylpyridine ligand shifts all redox potentials to a more negative (cathodic) potential, when compared to the parent complex Ir(pppy)₃ ($E_{1/2} = 0.77$ V/SCE).^{5a} In the conditions used (window of measurements: $+1.60 < E < -1.80$ V), it is not possible to observe the reduction waves, which are very probably localized on the pppy ligands.²¹

Optical Absorption. The data for the absorption spectra are summarized in Table 1, together with the oxidation potentials. In Figure 5, the absorption spectrum and luminescence profiles for *fac*- Δ -Ir(pppy)₃, are illustrated.

The absorption properties are discussed with reference to results for facial isomers of the Ir(III)-phenylpyridine complexes reported in the literature.^{1,3–6,22} The spectra show intense bands appearing between 240 and 350 nm which are assigned to spin allowed $\pi \rightarrow \pi^*$ transitions in the pppy ligand. At lower energies (into the visible region from 350 to 500 nm), weaker bands are observed. The assignment of these bands is more difficult, because their low intensity ($\epsilon \leq 10^4 \text{ M}^{-1} \text{ cm}^{-1}$, see Table 1 and Figure 5) is not compatible with spin allowed $\pi \rightarrow \pi^*$ transitions. On the other hand, MLCT transitions are also unlikely in this energy region, based on the fact that ligand centered reduction, if any, occurs at very negative potentials (see Table 1).²¹ In addition, careful inspection of the absorption profile in Figure 5, reveals structured features in the visible region, whereas MLCT bands are always structureless.^{1,23} It seems reasonable therefore to admit a mixed (LC–CT) character

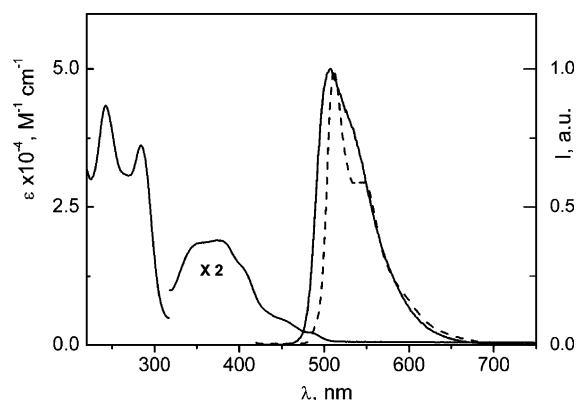


Figure 5. Absorption spectrum and normalized luminescence spectra of *fac*- Δ -Ir(pppy)₃ in degassed acetonitrile at 298 K (solid line), and at 77 K (dashed line).

Table 2. Luminescence and Photophysical Properties of the Iridium Complexes^a

	298 K								77 K	
	λ_{max} (nm)	$10^2 \times \Phi^{\text{air}}$	τ^{air} (ns)	$10^5 \times k_f$ (s ⁻¹)	Φ	τ (μs)	$10^5 \times k_f$ (s ⁻¹)	$10^5 \times k_{\text{nr}}$ (s ⁻¹)	λ_{max} (nm)	τ (μs)
Λ -Ir(pppy) ₃	505	0.9	19.4	4.6	0.64	1.4	4.6	2.6	507	2.1
Δ -Ir(pppy) ₃	507	1.0	20.5	4.9	0.64	1.6	4.1	2.3	511	2.3
Λ -IrL	508	1.0	24.5	4.1	0.51	1.2	4.2	4.1	507	1.9

^a Acetonitrile solvent, air-equilibrated and degassed cases as indicated. Excitation wavelength was 350 nm for luminescence spectra and 375 nm for luminescence lifetimes.

to these bands, by considering the possibility of intraligand CT transitions involving the phenyl and pyridyl rings of pppy ligand, as suggested by recent results for Ir(III) diphenylpyridine complexes.²⁴ Furthermore, for the tail extending further toward lower energy ($\epsilon \leq 10^3 \text{ M}^{-1} \text{ cm}^{-1}$), spin–orbit effect due to the metal center could be involved, leading to direct singlet-to-triplet transitions. The bands of *fac*- Λ -IrL are very close in energy to that of *fac*- Λ -Ir(pppy)₃, indicating that there are no important differences in coordination geometry in the two complexes. Both complexes exhibit strong LC absorption in the 300-nm region, indicating again a substantial similarity between bridged and unbridged pppy ligand.

Luminescence. Figure 5 compares the luminescence spectral profiles for complex *fac*- Δ -Ir(pppy)₃ in degassed acetonitrile at room temperature and at 77 K; the excitation wavelength was 350 nm. Quite similar spectra were obtained also for *fac*- Λ -Ir(pppy)₃ and *fac*- Λ -IrL.

The luminescence profiles in Figure 5 exhibit a vibronic resolution which is typical for the family of Ir(III)-ppy complexes;^{1,4–6,22} owing to the known temperature effect, the profiles at 77 K are better resolved than those at room temperature. It is noteworthy that the band maximum for the 77 K spectrum in Figure 5 is slightly red-shifted with respect to that at room temperature. This is in contrast with cases where the luminescence is of ³MLCT nature, as for example for the extensively studied Ru(II)-polypyridine complexes,²³ or for ³LC states with some admixture of ³MLCT character, as for example Ir(III)-terpyridine complexes.²⁵ Actually, for MLCT emitters, a typical blue-shifting is observed on going from room temperature (fluid solvent) to 77 K (frozen solvent).²³ On the basis

(21) Kulikova, M. V.; Balashev, K. P.; Kvam, P. I.; Songstad, J. *Russ. J. Gen. Chem.* **2000**, *70*, 163–170.

(22) Lamansky, S.; Djurovich, P.; Murphy, D.; Abdel-Razzaq, F.; Lee, H.-E.; Adachi, C.; Burrows, P. E.; Forrest, S. R.; Thompson, M. E. *J. Am. Chem. Soc.* **2001**, *123*, 4304–4312.

(23) Juris, A.; Balzani, V.; Barigelli, F.; Campagna, S.; Belser, P.; Von Zelewsky, A. *Coord. Chem. Rev.* **1988**, *84*, 85–277.

(24) Polson, M.; Fracasso, S.; Bertolasi, V.; Ravaglia, M. Scandola, F. *Inorg. Chem.* **2004**, *42*.

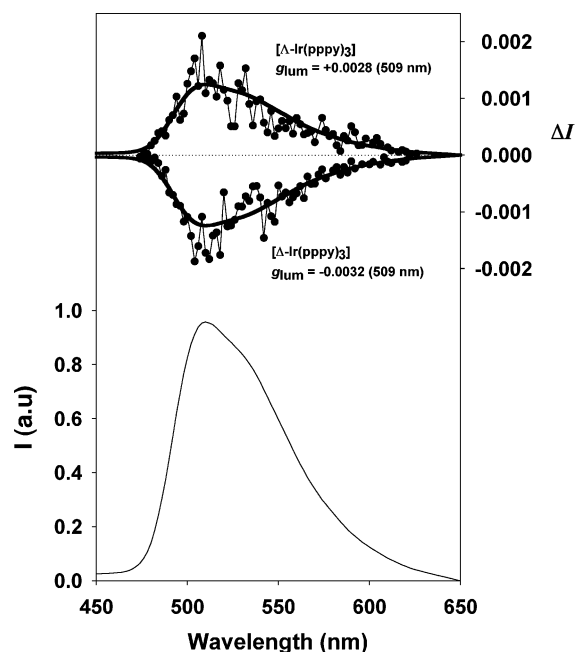


Figure 6. Circularly polarized luminescence (upper curve) and total luminescence (lower curve) spectra of the two Ir(III) complexes in dry MeCN at 295 K, upon excitation at 388 nm.

of these characteristics, the luminescence spectra for *fac*- Δ -Ir(pppy)₃ (and for *fac*- Λ -Ir(pppy)₃ and *fac*- Λ -IrL as well) are assigned to (largely) ³LC excited states. Table 2 collects luminescence data for both freeze–pump–thaw degassed, and air-equilibrated cases at room temperature and at 77 K in frozen solvent.

The complexes are highly luminescent in oxygen-free solvent, with luminescence quantum yields $\Phi \approx 0.5$ – 0.6 , and lifetimes $\tau \approx 1.2$ – $1.6 \mu\text{s}$. k_f and k_{nr} values are in the range 4 – 5×10^5 and 2 – $4 \times 10^5 \text{ s}^{-1}$, respectively, in line with previous results for complexes of the [Ir(ppy)₃] family.^{4–6,22} In air-equilibrated solvent, a remarkable quenching effect is registered, with $\Phi^{\text{air}} \approx 0.01$ and $\tau^{\text{air}} \approx 20 \text{ ns}$, a 60-fold reduction in luminescence features with respect to degassed solutions. The luminescence of the complexes is quenched by dioxygen with a rate that can be drawn from the data of Table 2, on the basis of the equation below.²⁶

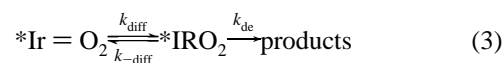
$$\frac{\tau}{\tau^{\text{air}}} = \frac{\Phi}{\Phi^{\text{air}}} = 1 + k_q \tau [\text{O}_2] \quad (1)$$

The evaluated value for $k_q[\text{O}_2]$ for the three investigated complexes is $4.9 \pm 0.2 \times 10^7 \text{ s}^{-1}$. Given that for air-equilibrated acetonitrile, $[\text{O}_2] = 1.9 \times 10^{-3}$,²⁷ the evaluated average quenching rate constant is $k_q = 2.6 \pm 0.2 \times 10^{10} \text{ M}^{-1} \text{ s}^{-1}$. This appears to be among the highest values ever reported for quenching of luminescence of transition metal complexes by dioxygen; for comparison purposes, k_q is ca. 2×10^9 for both [Ru(bpy)₃]²⁺,²⁸ and [Os(bpy)₃]²⁺,²⁹ and $1.1 \times 10^8 \text{ M}^{-1} \text{ s}^{-1}$, for

[Ir(tpy)₂]³⁺.²⁵ To notice that for acetonitrile solvent, the diffusion constant is $k_{\text{diff}} \approx 2.0 \times 10^{10} \text{ M}^{-1} \text{ s}^{-1}$, as evaluated from equation below³⁰

$$k_{\text{diff}} = \frac{8RT}{3\eta} 1000 \quad (2)$$

where R is the gas constant and $\eta = 0.345 \times 10^{-3} \text{ Pa s}$ ³⁰ is the solvent viscosity. The fact that for our Ir-tris-cyclometalated complexes, the observed quenching rate constant is approximately equal to the diffusion constant, indicates that the quenching step within the collision associate is highly efficient, eqs 3 and 4³⁰



$$k_q = \frac{k_{\text{diff}} k_{\text{de}}}{k_{-\text{diff}} + k_{\text{de}}} \quad (4)$$

where $*\text{Ir}$ stands for the luminescent triplet of the iridium complex, $*\text{Ir} \cdots \text{O}_2$ is the collision associate, $k_{-\text{diff}}$ is the rate for break up of the collision associate into the original species, and k_{de} is the rate constant for product formation from the associate. Thus, for $k_{\text{de}} \gg k_{-\text{diff}}$, $k_q \approx k_{\text{diff}}$. This is in contrast with what happens for most cases of luminescence quenching in several metal complexes, where k_q was found to be well lower than k_{diff} , and where energy transfer (occurring with efficiencies lower than unit) was the predominant mechanism associated with k_{de} .²⁸

The energy content of $*\text{Ir}$ is ca. 2.4 eV, as estimated from the emission profiles, and the quenching mechanism for the couple $*\text{Ir}/\text{O}_2$ could involve an energy transfer or an electron-transfer process.²⁸ Energy transfer would lead to a singlet oxygen state (¹O₂), and for the present cases would be exothermic by about 1–1.5 eV (1.6 and 1.0 eV are the energy levels of the two available excited states of the oxygen species).^{31,32} In conclusion, when energy transfer takes place, k_q is found no more than 2 – $4 \times 10^9 \text{ M}^{-1} \text{ s}^{-1}$ in acetonitrile,^{25,28,29,32} while it is found an outstanding $k_q = 2 \times 10^{10} \text{ M}^{-1} \text{ s}^{-1}$ in our complexes. For these, the driving force for an electron-transfer step within the couple $*\text{Ir}/\text{O}_2$, can be evaluated to be $\Delta G^\circ \approx -1.1 \text{ eV}$ (2.4 eV is the energy content of $*\text{Ir}$, oxidation of our Ir complexes and reduction of oxygen are $\sim +0.53$ and -0.78 V vs SCE, respectively). Interestingly, the reorganization energy for electron transfer in acetonitrile, λ , is between 0.6 and 1 eV, as evaluated according to current approaches.³³ Thus, it seems that the activation energy for electron transfer within the $*\text{Ir}/\text{O}_2$ couple, eq 5³³

$$\Delta G^* = \frac{\lambda}{4} \left(1 + \frac{\Delta G^0}{\lambda} \right)^2 \quad (5)$$

can be close to zero (i.e., photoinduced electron transfer within $*\text{Ir}/\text{O}_2$ could be barrierless). In conclusion, the occurrence of

- (25) Collin, J.-P.; Dixon, I. M.; Sauvage, J.-P.; Williams, J. A. G.; Barigelletti, F.; Flamigni, L. *J. Am. Chem. Soc.* **1999**, *121*, 5009–5016.
 (26) Lakowicz, J. R. *Principle of Fluorescence Spectroscopy*; Plenum Publishers: New York, 1999; Vol. 8.
 (27) Murov, S. L.; Carmichael, I.; Hug, G. L. *Handbook of Photochemistry*; New York, 1993.
 (28) (a) Demas, J. N.; Harris, E. W.; McBride, R. P. *J. Am. Chem. Soc.* **1977**, *99*, 3547–3551. (b) Abdel-Shafi, A. A.; Beer, P. D.; Mortimer, R. J.; Wilkinson, F. *Helv. Chim. Acta* **2001**, *84*, 2784–2795.

- (29) The luminescence lifetime for [Os(bpy)₃]²⁺ in degassed and air-equilibrated acetonitrile is 65 and 50 ns, respectively.
 (30) Murov, S. L.; Carmichael, I.; Hug, G. L. *Handbook of Photochemistry*; New York, 1993, pages 207–209.
 (31) Halliwell, B.; Gutteridge, J. M. C. *Free Radical in Biology and Medicine*; Clarendon: Oxford, 1982.
 (32) Abdel-Shafi, A. A.; Beer, P. D.; Mortimer, R. J.; Wilkinson, F. *Phys. Chem. Chem. Phys.* **2000**, *2*, 3137–3144.
 (33) (a) Marcus, R. A.; Sutin, N. *Biochim Biophys. Acta* **1985**, *811*, 265–322. (b) Wasielewski, M. R. In *Photoinduced Electron Transfer, Part A*; Fox, M. A., Chanon, M. Eds.; Elsevier: Amsterdam, 1988, 161–206.

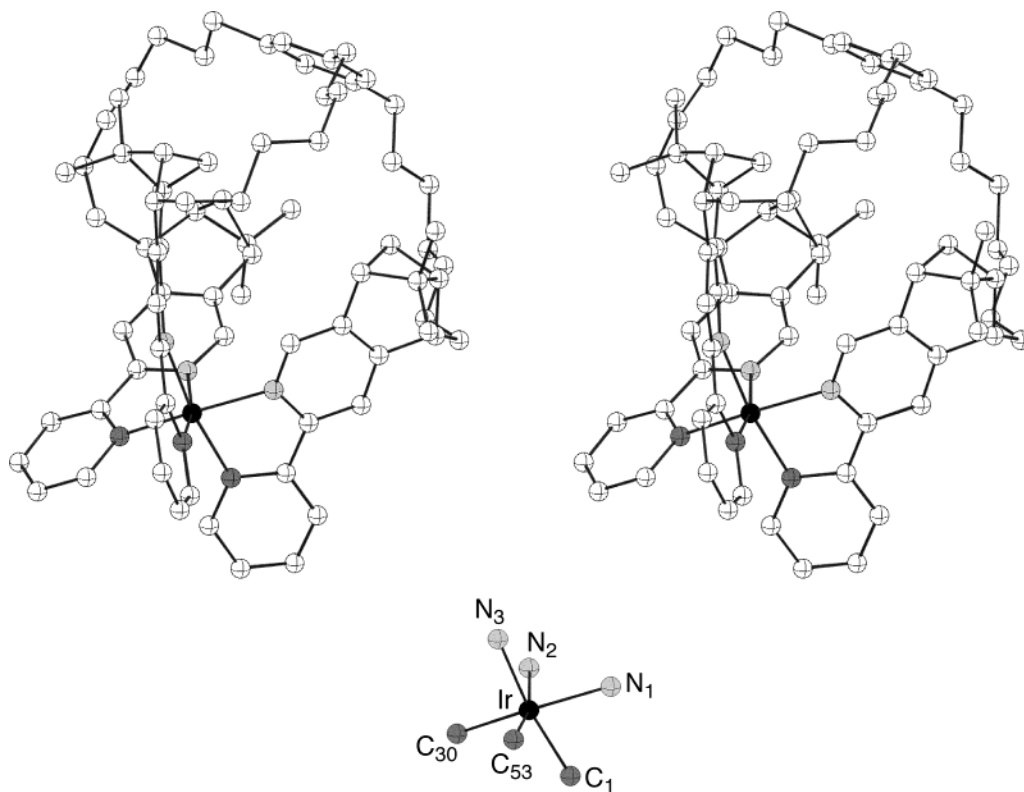


Figure 7. Stereopair of the X-ray structure of *fac*- Δ -IrL. The hydrogen atoms are omitted for clarity. Selected bond lengths (Å) and bond angles (deg) are: Ir–N1, 2.140(5); Ir–N2, 2.133(5); Ir–N3, 2.120(5); Ir–C1, 2.012(7); Ir–C30, 2.026(8); Ir–C53, 2.001(6); C53–Ir–N3, 79.5(2); C30–Ir–N2, 79.5(3); C1–Ir–N1, 79.6(2); C53–Ir–N2, 169.8(2); C1–Ir–N3, 167.0(2); C30–Ir–N1, 169.3(3).

electron transfer might provide a possible explanation for the very high k_q obtained experimentally.

Circularly Polarized Luminescence (CPL) Measurements.

The circularly polarized luminescence (ΔI) and total luminescence (I) spectra measured for *fac*- Δ -Ir(pppy)₃ and *fac*- Λ -Ir(pppy)₃ in acetonitrile solutions (at 295 K) are shown in Figure 6.

The degree of circularly polarized luminescence is given by the luminescence dissymmetry ratio

$$g_{\text{lum}} = \frac{\Delta I}{I} = \frac{I_L - I_R}{I_L + I_R} \quad (6)$$

where I_L and I_R refer, respectively, to the intensity of left and right circularly polarized emissions. As usual for most chiral organic chromophores and transition metal complexes,³⁴ $|g_{\text{lum}}|$ that were obtained are small: -0.0032 ± 0.0004 for *fac*- Δ -Ir(pppy)₃ and $+0.0028 \pm 0.0004$ for *fac*- Λ -Ir(pppy)₃ as determined at the maximum emission wavelength. Although the g_{lum} values are very small (a value equal to ~ 0.003 corresponding to light that is only 0.3% circularly polarized), opposite CPL signals were measured for the two compounds having opposite configuration at the metal center. Indeed, it is usually assumed that the sign and the magnitude of the CPL signals are mainly determined by the Δ or Λ arrangement of the ligands. Remote asymmetric centers on the ligands have little direct effect on

the observed spectra, but “cause” CPL or CD due to their influence on chiral coordination. To our best knowledge, this is the first example of CPL from iridium (III) complexes and, although the signals here are weak, they are measurable.

X-ray Structure Analysis. The crystal structure of the iridium complex *fac*- Λ -IrL confirms the formation of the neutral 1:1 complex. The compound crystallizes in the chiral space group $P2_12_12$ (Flack parameter $x = -0.003(7)$) with one neutral complex molecule and 1.5 acetone molecules (partially occupied) per asymmetric unit. A view of the complex is shown in Figure 7. The structure shows nicely the coiling of the tris-cyclometalating ligand **L** around the Ir(III) center. The three cyclometalating moieties coordinate in an octahedral coordination geometry. The complex has approximate C_3 -symmetry (not crystallographic) with Ir–N and Ir–C bond lengths in the range 2.120(5)–2.140(5) and 2.001(6)–2.026(8), respectively. These values are similar to those reported for the *fac*-Ir(tpy)₃ (tpy = 2-(para-tolyl)pyridine) complex.³⁵ The bite angles within each chelate are around 79.5° and the torsional angles N–C–C–C range between 6.9(14)° and 11.1(8)° indicating a small deformation from planarity of the phenylpyridine units.

Conclusion

This report represents a further step in the systematic development of stereoselective synthesis of coordination compounds. It shows clearly that the introduction of chiral centers in the ligands, in this case the pinene groups attached to the pyridine ring of phenylpyridine, leads to only modest stereoselectivity with respect to helical configuration of the octahedral

(34) (a) Riehl, J. P.; Richardson, F. S. *Chem. Rev.* **1986**, *86*, 1–16. (b) Peacock, R. D.; Stewart, B. *J. Chem. Soc., Chem. Commun.* **1982**, 295–296. (c) Gunde, K. E.; Credi, A.; Jandrasics, E.; von Zelewsky, A.; Richardson, F. S. *Inorg. Chem.* **1997**, *36*, 426–434. (d) Field, J. E.; Muller, G.; Riehl, J. P.; Venkataraman, D. *J. Am. Chem. Soc.* **2003**, *125*, 11 808–11 809.

(35) Garces, F. O.; Dedian, K.; Keder, N. L.; Watts, R. J. *Acta Crystallogr.* **1993**, *C49*, 1117–1120.

Ir(III)-center in a tris-didentate cyclometalated complex. Connecting these three ligands by a C_3 -symmetric moiety (derived from mesitylene) yields a chiral tripod ligand that coordinates in a completely stereoselective way to the Ir(III)-center. The introduction of the pinene groups into the ligand has, beside the stereo control, the benefit of rendering these uncharged molecules highly soluble in a large range of solvents. Their photophysical properties are an additional feature of this interesting class of compounds.

Acknowledgment. We thank Freddy Nydegger (University of Fribourg) for the electrospray mass spectra, the Swiss

National Science Foundation and the FIRB project RBNE019H9K “Molecular Manipulation for Nanometric Devices” by MIUR for financial support. This work is dedicated to the memory of Jean-Marc Kern.

Supporting Information Available: Tables of crystal data, atomic coordinates, bond distances, bond angles and anisotropic displacement parameters for *fac*- Λ -IrL, as well as the CIF file. This material is available free of charge via the Internet at <http://pubs.acs.org>.

JA048655D